IAOS

International Association for Obsidian Studies

Bulletin

ISSN: 2310-5097

Number 57 **Summer 2017**

CONTENTS

International Association for Obsidian Studies

President	Rob Tykot
President Elect	Kyle Freund
Secretary-Treasurer	Matt Boulanger
Bulletin Editor	Carolyn Dillian
Webmaster	Craig Skinner

Web Site: http://members.peak.org/~obsidian/

NEWS AND INFORMATION

NEWS AND NOTES

Have news or announcements to share? Send them to IAOS.Editor@gmail.com for the next issue of the *IAOS Bulletin.*

CONSIDER PUBLISHING IN THE IAOS *BULLETIN*

The *Bulletin* is a twice-yearly publication that reaches a wide audience in the obsidian community. Please review your research notes and consider submitting an article, research update, news, or lab report for publication in the *IAOS Bulletin*. Articles and inquiries can be sent to IAOS.Editor@gmail.com Thank you for your help and support!

CONFERENCES

Look inside for announcements of two upcoming conferences of interest to IAOS members. From November 7-12, 2017, the 11th International Conference on Knappable Materials will be held in Argentina; and an early announcement for the International Obsidian Conference to be held May 27-29, 2019 in Hungary. See details in this issue of the *IAOS Bulletin.*

NOTES FROM THE PRESIDENT-ELECT*

Greetings from sunny Florida! I'll begin by expressing my gratitude to all of those who voted in the IAOS election. Although there was a limited field, your support is much appreciated and I look forward to serving in the upcoming years. It was really great to see many of you this past April in Vancouver for the SAA Annual Meeting. Having lived in Canada for several years, this was a welcome return to the land of maple syrup and loonies and toonies. At the IAOS meeting we discussed the success of the International Obsidian Conference held last year in Lipari, Italy and our excitement for the next one being held in Hungary in 2019. Being part Hungarian myself, I'm looking forward to a new cultural experience - and of course visiting the Carpathian obsidian sources.

Summer is always a hectic time when many of us are in the field or feverishly trying to catch up on backlogged projects. For me, this summer has been no different. I recently finished putting together a manuscript on the long-term exploitation of Lipari obsidian, a paper that builds upon my dissertation and extensive work on prehistoric obsidian consumption in ancient Sicily. I also found time to get to Sardinia, where I was able to export a selection of metal slags for SEM analysis. The adoption of metalworking in this region appears to have been a driving force in the reconfiguration of long-standing obsidian exchange networks, and this work is part of a larger project exploring the Neolithic-Chalcolithic transition and the intersections between obsidian and early metal technology.

Separate from my work in the Mediterranean, I also just returned from a conference on cemetery resource protection. You heard right! Last year I begin working in collaboration with the Florida Public Archaeology Network (FPAN) on the Florida Historic Cemetery Recording Project (FLHCRP). This is now a formal class at IRSC in which students are systematically recording gravemarkers in historic cemeteries as a means of studying the diverse ways in which various cultural groups have commemorated those who have passed. This type of research and fieldwork is certainly a new challenge for me, but I have found it particularly rewarding. I even had the opportunity to discuss our work as part of a National Public Radio (NPR) segment.

Have a great summer!

Kyle Freund, IAOS President-Elect
Department of Anthropology
Indian River State College
kfreund@irsc.edu

*Editor's Note: Though this is typically a space for comments from our IAOS President, we are pleased to introduce our IAOS President-Elect with this issue of the *IAOS Bulletin*. Dr. Freund will step into the role of President beginning in the spring of 2018. Congratulations!

First Announcement

International Obsidian Conference 2019

27–29 May 2019,

Budapest and Sárospatak (Hungary)

IOC 2019

Dear colleagues,
We invite you to participate in the next International Obsidian Conference, in May 2019 in Hungary, Budapest and Sárospatak

The conference is intended as consecutive to the Lipari Obsidian Conference held in 2016 (http://rtykot.myweb.usf.edu/Obsidian%202016/).

The meeting's programme will include issues related to different fields of obsidian studies – archaeology, geology, anthropology, and archaeometry. The meeting's venue in Budapest is the Hungarian National Museum and in Sárospatak the Rákóczi Museum of the HNM.

The registration fee is **100 € (125 US $) for professionals, and 50 € (65 US $) for students.** Early bird registration fee is **80 € (100 US $) and 40 € (50 US $),** respectively. Transport and accommodation facilities will be communicated on our website (http://ioc-2019.ace.hu/). You can already use our Pre-registration form to be kept personally informed (http://ioc-2019.ace.hu/node/15). Formal registration will start in May 2018.

The planned sessions of the Conference are the following:

- Formation and geology of obsidian
- Sources and their characterisation
- Analytical / methodological aspects of obsidian studies
- Archaeological obsidian by chronological periods
- Lithic technology and use wear
- Theoretical and cultural anthropological issues

Your ideas concerning other sessions are welcome!

Contact organisers at: tbk@ace.hu (Katalin T. Biró)
markoa@hnm.hu (András Markó)

Partner institutions

- HNM Rákóczi Museum (HNM-RM), Sárospatak, Hungary
- Eötvös Loránd University (ELU), Budapest, Hungary
- Centre for Energy Research, Hungarian Academy of Sciences (MTA EK), Budapest, Hungary
- Hungarian Geological and Geophysical Institute (MFGI)
- Hungarian Natural History Museum, Budapest, Hungary (HNHM)
- Herman Ottó Museum (HOM), Miskolc, Hungary
- State Geological Institute of Dionýz Štúr (SGI), Bratislava, Slovakia
- Institute of Archaeology, Slovak Academy of Sciences (IA), Nitra, Slovakia
- Masaryk University (MU), Brno, Czech Republic
- Taras Shevchenko National University (TSNU), Kyiv, Ukraine
- Ferenc Rákóczi II. Transcarpathian Hungarian Institute (KMF), Beregovo, Ukraine

Organiser of the Conference

- Hungarian National Museum (HNM)

Local Organising Committee

- T. Biró Katalin – HNM
- Markó András – HNM
- Kasztovszky Zsolt – MTA EK
- Weiszburg Tamás – ELU
- Csengeri Piroska – HOM
- Péterdi Bálint – MFGI
- Papp Gábor – HNHM
- Rajczy Miklós – HNHM
- Tamás Edit – HNM-RM
- Zuzana Bačová & Pavel Bačo – SGI
- Ľubomíra Kaminská – IA
- Antonín Přichystal – MU
- Rácz Béla – KMF
- Sergei Ryzhov – TSNU

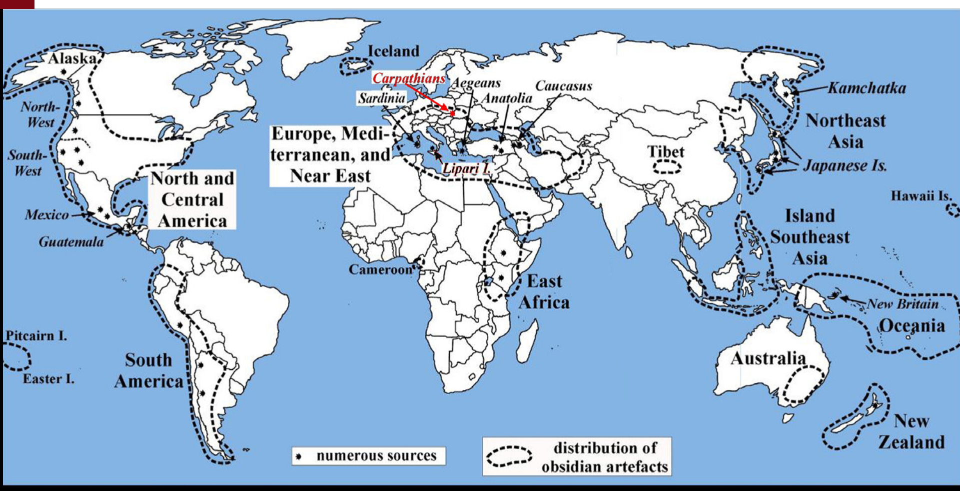

Scientific Committee

- Akira Ono – Meiji University, Tokyo, Japan
- Michael Glascock – University of Missouri, Columbia, MO, USA
- Yaroslav Kuzmin – Institute of Geology & Mineralogy, Siberian Branch of the Russian Academy of Sciences, Novosibirsk, Russia
- Robert Tykot – University of South Florida, Tampa, FL, USA
- Robin Torrence – Australian Museum, Sydney, Australia
- François-Xavier Le Bourdonnec – Université Bordeaux Montaigne, Pessac, France
- Jaroslav Lexa – Earth Sciences Institute of the Slovak Academy of Sciences, Bratislava, Slovakia

11th INTERNATIONAL SYMPOSIUM ON KNAPPABLE MATERIALS

"From toolstone to stone tools"

Buenos Aires and Necochea (Argentina), November 7-12th, 2017

Second Announcement - Call for Abstracts

Dear friends and colleagues

We have been working on the sessions proposals received and we are happy to announce that there are 11 sessions which cover a wide range of topics. We believe the symposium will lead to some very interesting and fruitful discussions. Hence, we invite you to send your abstracts. Please find the list of sessions at the end of this announcement.

Abstracts should not exceed 200 words in length each, should be 1.5 spaced with 2.5 cm margins on all sides, and use Verdana font, 12 point. The title should be centred and in bold letters. The full name(s), institutional affiliation(s) and email address(es) of the author(s) should be included as footnotes, left aligned.

When you send your abstract, please choose the session you will be presenting your paper at and indicate if the presentation will be given online (a distance presentation) or in person (attending the symposium). Abstracts must be sent to the organizers of the session and also to the official email address of the symposium (11iskm2017@gmail.com).

The deadline for submitting abstracts is **May 15th, 2017**. The abstracts received will be evaluated by the Organizing Committee and sessions organizers and, if there are any changes to make, we will let you know by June 1st. The final list of presentations will be made afterwards in a future announcement.

We would like to remind you that English is the official language of the symposium.

WE LOOK FORWARD TO SEEING YOU AT THE SYMPOSIUM!

Contact us at:

11iskm2017@gmail.com

Look for us at:

http://www.imhicihu-conicet.gov.ar/iskm2017/

https://www.facebook.com/11thInternationalSymposiumonKnappableMaterials/

Organizing Institution

IMHICIHU
CONICET

Scientific Committee

Daniel S. Amick (Loyola University Chicago), **Astolfo Araujo** (Universidade de São Paolo), **Carlos Aschero** (CONICET-Universidad de Tucumán), **Cristina Bellelli** (CONICET-INAPL and Universidad de Buenos Aires), **Eric Boëda** (Université Paris Ouest-CNRS), **Luis Alberto Borrero** (CONICET-IMHICIHU and Universidad de Buenos Aires), **Laurenz Bourguignon** (Institut National de Recherches Archéologiques Préventives, France), **Adrián Burke** (Université de Montréal), **Phillip Carr** (University of South Alabama), **María Teresa Civalero** (CONICET-INAPL and Universidad de Buenos Aires), **Valeria Cortegoso** (CONICET-LPEH and Universidad Nacional de Cuyo), **Otis Crandell** (Universidade Federal do Paraná, Brazil), **Patricia Escola** (CONICET-Universidad Nacional de Catamarca), **Nora Flegenheimer** (CONICET-Área de Arqueología Municipalidad de Necochea), **Nora Franco** (CONICET-IMHICIHU and Universidad de Buenos Aires), **Michael Glascock** (University of Missouri), **Kelly Graf** (Texas A&M University), **Patrick Julig** (Laurentian University, Canada), **Xavier Mangado** (Universidad de Barcelona), **Estela Mansur** (CONICET and

Universidad Nacional de Tierra del Fuego), **César Méndez Melgar** (Universidad de Chile), **Hugo Nami** (CONICET), **Yoshi Nishiaki** (University of Tokyo), **Ryan Parish** (University of Memphis), **Marta Sánchez de la Torre** (Institut de Recherche sur les Archéomatériaux–Centre de Recherche en Physique appliquée à l'Archéologie, IRAMAT–CRP2A), **Charles Stern** (University of Colorado, Boulder) and **Robin Torrence** (Australian Museum, Sydney).

Organizing Committee

Nora Franco (CONICET-IMHICIHU and Universidad de Buenos Aires), **Karen Borrazzo** (CONICET-IMHICIHU and Universidad de Buenos Aires), **Jimena Alberti** (CONICET-IMHICIHU), **Silvana Buscaglia** (CONICET-IMHICIHU), **Analía Castro** (CONICET-INAPL), **Alejandra Elías** (CONICET–INAPL), **Mariano Colombo** (Área de Museos de la Municipalidad de Necochea), **Natalia Mazzia** (CONICET-Área de Arqueología Municipalidad de Necochea), **Celeste Weitzel** (CONICET-Área de Arqueología Municipalidad de Necochea), **Agueda Caro Petersen** (Museo de Ciencias Naturales, Necochea), **Daniel Hereñú** (CONICET-IMHICIHU).

STEADY-STATE HYDRATION AND PROTOCOLS FOR INDUCED HYDRATION OF OBSIDIAN

Alexander K. Rogers
Maturango Museum

Abstract
Induced hydration is a frequently-used method of determining hydration rates of obsidian, in which hydration is measured at elevated temperatures and mathematically related to archaeological temperatures. It has the advantage that it is not subject to the error sources which plague hydration rates based on association with radiocarbon or temporally-sensitive artifacts. However, on occasion the induced hydration method yields incorrect hydration rates, particularly when abbreviated hot-soak times are used. Obsidian seems to undergo a transient state when hydration begins, and a finite time interval is required to reach steady state hydration; measurements made before this will yield incorrect results. This paper proposes a simple equation for estimating the hot-soak times required in an induced hydration protocol.

Introduction

Induced hydration is based on the principle that the temperature dependence of hydration rate is known. Obsidian can be hydrated at elevated temperatures, at which measurable hydration rims form rapidly; analysis of these measurements then allows computation of hydration rate at archaeological temperatures. Induced hydration has the advantage that the hydration rate is determined entirely by laboratory methods. Other methods require associating obsidian with other temporal data such as radiocarbon or temporally-sensitive artifacts, and hence are subject to association errors.

However, on occasion the induced hydration method yields incorrect hydration rates (Rogers and Duke 2014), particularly when abbreviated hot-soak times are used. There is a strong motivation to use hot-soak times which are as short as possible, to avoid tying up laboratory equipment any longer than necessary, so the standard protocol employs relatively short hydration times which are just sufficient to develop measurable hydration rims. The incorrect results seem to be the result of a transient phase at the initiation of the hot-soak process, and do not arise if longer hot-soak times are used (Rogers and Duke 2011). This paper proposes a simple model of the transient phase as a guide for designing induced hydration profiles.

Obsidian Hydration

"Obsidian hydration", in its most basic aspect, describes the process by which water is absorbed by obsidian, and involves both physical and chemical changes in the glass (Doremus 2002; Anovitz et al. 2008). When a fresh surface of obsidian is exposed to air, water molecules adsorb on the surface. Since any unannealed obsidian surface exhibits cracks at the nano-scale, the amount of surface area available for adsorption is much greater than the macro-level surface area would suggest, creating a large surface concentration. Some of the adsorbed water molecules, plus others impinging directly from the atmosphere, are absorbed into the glass and diffuse into the inter-atomic spaces in the glass matrix. The diffusion process is driven primarily by the water concentration gradient, and resisted by the viscosity of the glass. The diffusing molecules stretch the glass matrix, causing an increase in volume in the hydrated region; they also cause an increase in the openness of the glass matrix itself, facilitating further absorption of water. Since the hydrated region is expanded and the non-hydrated region is not, a stress region exists between the two. As time passes, the region of increased water concentration progresses into the glass, its rate being a function of the initial openness of the glass, temperature, and the dynamics of the process itself. When the hydrated layer becomes thick enough, typically greater than 20 microns, the accumulated stresses cause the layer to spall off as perlite.

The classical field of obsidian hydration dating (OHD) is based on measuring the position of the stress zone caused by the diffusion process. The interface between the hydrated and unhydrated volumes is a zone of optical contrast when observed under polarized light, due to the phenomenon of "stress birefringence" (Born and Wolf 1980, 703-705). The position of the stress region proceeds into the glass with the square root of time (Doremus 2002):

$$r^2 = k*t \qquad (1)$$

where r is the hydration rim thickness, t is time, and k is the hydration rate. The hydration rate also varies with temperature as described by the Arrhenius equation

$$k = A*\exp(-E/(R*T)) \qquad (2)$$

where E is the activation energy, A is the pre-exponential, R is the universal gas constant (8.314 j/mol°K), and T is temperature in °K (Doremus 2002). Below the glass transition temperature the activation energy and pre-exponential are independent of temperature. This temperature dependence is the basis of induced hydration, and the validity of the method depends on the validity of equation (2).

Induced Hydration

To perform induced hydration, a set of specimens is first prepared. A number of flakes (in this case five) are removed from the same piece of obsidian; each flake is placed in a pressure vessel with distilled water, to which silica gel is added to create a saturated solution. The purpose of the silica gel is to prevent chemical erosion of the surface of the obsidian, which is otherwise attacked by the hot water bath. Alternatively, the specimens can be suspended in a vapor bath, above the water surface; in this case the silica gel is not needed.

The pressure vessel is then placed in a laboratory oven with a laboratory-grade temperature controller, and the temperature quickly raised to the hot-soak temperature specified. After the length of time prescribed by the experimental protocol for that temperature, the pressure vessel is removed from the oven, quickly cooled down, the specimen is removed and quenched, and the hydration rim measured. This measurement set (time, temperature, and hydration rim) constitutes one data point. The process is repeated with the other specimens at different temperatures and times. A detailed description is provided in Stevenson et al. 1998.

To analyze the data, equations (1) and (2) are combined to give

$$r^2/t = A*\exp(-E/(R*T)) \qquad (3)$$

Taking the natural logarithm of both sides gives the logarithmic Arrhenius equation

$$\ln(r^2/t) = \ln(A) - (E/R)*(1/T) \qquad (4)$$

If we define

$$Y = \ln(r^2/t) \qquad (5)$$

and

$$X = 1/T \qquad (6)$$

then equation (4) is a linear equation of the form

$$Y = I + S*X \qquad (7)$$

with I = ln(A) and S = -E/R. Equation (7) can then be solved for I and S by linear least-squares methods (Cvetanovic et al. 1979).

Transient Phase Model

There are indications that, in some circumstances, the hydration rate is not constant with time at constant temperature (Stevenson and Novak 2011; Rogers and Duke 2014); equation (2) is thus not valid for these cases and the induced hydration method fails. The reason for this is not clear, but appears to be due to a period of transient behavior before hydration reaches a steady state.

The observable hydration rim is the result of stress between the hydrated and unhydrated volumes, as the glass in the hydrated region expends due to slight depolymerization caused by the absorbed water. The progress of the stress region is driven by the water concentration gradient, and resisted by the viscosity of the glass, which decreases with increasing water content and with increasing temperature (Doremus 1994). Experimental data suggest there is a period of transient behavior when hydration first starts, followed by a steady state hydration condition (Rogers and Duke 2014; Stevenson and Novak 2011; Stevenson and Rogers 2015). Induced hydration measurements made within this transient phase will not be representative of steady-state conditions and will yield incorrect rates.

Few data have been published, but it appears that, for Napa Glass Mountain obsidian at 90°C, steady state is achieved after approximately 90 – 110 days, while for Meadow Valley Mountains obsidian at 140°C it occurs at about 40 – 50 days (Rogers and Duke 2014:433 Fig. 2, and 434 Fig. 3). Both obsidians have intrinsic total water of approximately 0.1 wt%; an obsidian with higher intrinsic water content would have lower viscosity and would be expected to reach steady state more rapidly.

A simple model can be developed based on the physics of viscosity in glass (Doremus 1994). Viscosity is described by an Arrhenius equation of the form

$$v = K_1 * \exp(Q/T) \quad (8)$$

where v is viscosity, K_1 is a pre-exponential constant, Q is activation energy, and T is absolute temperature. Over temperature ranges of interest in archaeology (i.e., much less than the glass transition temperature), K_1 and Q are essentially independent of temperature (Doremus 1994).

As a first-order model, assume the time of onset of the steady state hydration process occurs more rapidly at lower viscosities, that is, t_s is proportional to viscosity. Then

$$t_s = K_2 * \exp(Q/T) \quad (9)$$

where K_2 is a proportionality constant. By transforming equation (9) into logarithmic form, the values of K_2 and Q can be estimated from the Napa Glass Mountain and Meadow Valley Mountains data cited above.

$$\ln(t_s) = \ln(K_2) + Q/T \quad (10)$$

Setting t_s = 100 days @ 90°C (363.15°K) and t_s = 50 days @ 140°C (413.15°K), solution of equation (10) yields K_2 = 0.31 days and Q = 2100 °K, so

$$t_s = 0.31 * \exp(2100/T) \quad (11)$$

Both the obsidian specimens cited have intrinsic water content of approximately $\%H_2O_t$ = 0.1 wt%, so the pre-exponential is specific to one water concentration value.

Since viscosity decreases with increasing intrinsic water content (Friedman et al. 1963), the t_s values from equation (11) are conservative; use of them will yield steady state for specimens with higher water content, but may be unnecessarily long.

Since data for higher water content obsidians are lacking, a model is proposed based on the physics of the hydration process. A model of the hydration rate and its relationship to water content and temperature is

$$k=\exp(37.76–2.289*w – 10433/T + 1023*w/T) \quad (12)$$

where k is the hydration rate in μ^2/1000 years, w is total intrinsic water in wt%, and T is temperature in °K (Rogers 2015). The form of the equation is well attested in geophysics (Zhang et al. 1991; Zhang and Behrens 2000), although the values of the numerical parameters vary based on pressure and temperature conditions. The hydration process is clearly related to the viscosity, since viscosity is the force resisting absorption of water. Therefore I am going out on a limb and suggesting a similar form of equation for viscosity and hence for t_s, although again the numerical parameters may vary. Then the factor Q in equation (9) corresponds to the last two terms in equation (12), and the principal variation with w is in the second term. As a rough approximation, I propose a form for K_2 of

$$K_2 = 0.38*\exp(-2*w) \quad (13)$$

The prefactor of 0.38 causes K_2 to equal 0.31 when w = 0.1, agreeing with equation (11); the factor of 2 is a round-off of the factor of 2.289 in equation (12), since further precision is inappropriate without more experimental data. Thus the approximate form for the onset of steady state is

$$t_s = 0.38*\exp(-2*w + 2100/T) \quad (14)$$

with t_s in days, w in wt%, and T in °K.

Discussion

The model proposed in equation (14) can be used to compute minimum hot-soak times required for successful use of the induced hydration method. As an example, three cases are computed, for H_2O_t = 0.1, 0.6, and 1.0 wt%, corresponding to “dry”, “intermediate”, and ‘wet” obsidians. Archaeologically these are represented by, for example, Napa Glass Mountain, Coso West Sugarloaf, and Coso Sugarloaf mountain, respectively. Temperatures between 110 and 150°C are chosen, since they are standard hot-soak temperatures. Table 1 shows results, rounded off to the nearest whole day.

The standard hot-soak protocol today is 30 days @ 110°C, 25 days @ 120°C, 20 days @ 130°C, 15 days @ 140°C, and 10 days @ 150°C. Figure 1 presents the data of Table 1, with the standard protocol shown for comparison.

Figure 1 shows that the hot-soak times for the standard protocol are too short for “dry” obsidians, those with H_2O_t < 0.6 wt%; steady-state conditions will not be reached and erroneous computations of hydration rate will result (as in Rogers and Duke 2014).

The longer hot-soak times in Rogers and Duke (2011) resulted in a rate which agreed with archaeology for a similarly “dry” obsidian.

Temperature, °C	Hot-soak time in days, H_2O_t = 0.1 wt%	Hot-soak time in days, H_2O_t = 0.6 wt%	Hot-soak time in days, H_2O_t = 1.0 wt%
110	101	37	17
120	75	27	12
130	65	24	11
140	57	21	9
150	50	18	8

Table 1. Minimum hot-soak times

Conclusions

This analysis proposes a simple model for the time required for obsidian hydration to reach steady state. The model is useful in designing induced hydration protocols so as to avoid transient conditions and the associated errors in hydration rate. A strong caveat is that the model should be regarded as preliminary, and subject to revision as more data become available, especially for higher water content.

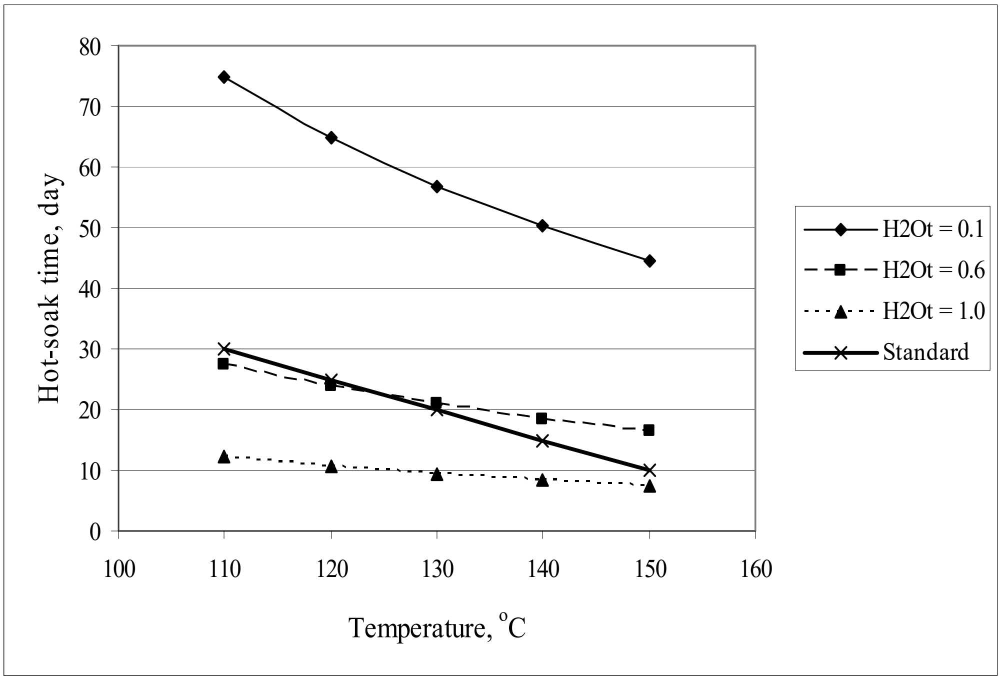

Figure 1. Minimum hot-soak times for induced hydration protocols, as a function of specimen intrinsic water content (%H_2O_t in wt%).

References Cited

Anovitz, L.M., D.R. Cole, and M. Fayek (2008) Mechanisms of Rhyolitic Glass Hydration below the Glass Transition. *American Mineralogist* 93:1166-1178.

Born, M., and E. Wolf (1980) *Principles of Optics*, 6th ed. Pergamon Press, New York.

Cvetanovic, R.J., D.L. Singleton, and G. Paraskevopoulos (1979) Evaluations of the Mean Values and Standard Errors of Rate Constants and their Temperature Coefficients. *Journal of Physical Chemistry* 83(1):50-60

.

Doremus, R.H. (1994) *Glass Science*. Wiley Interscience, New York.

Doremus, R.H. (2002) *Diffusion of Reactive Molecules in Solids and Melts*. Wiley Interscience, New York.

Friedman, I., W. Long, and R.L. Smith (1963) Viscosity and Water Content of Rhyolite Glass. *Journal of Geophysical Research 68*(34):6523-6535.

Rogers, A.K. (2015) An Equation for Estimating Hydration Rate of Obsidian from Intrinsic Water Concentration. *International Association for Obsidian Studies Bulletin,* 53: 5-13.

Rogers, A.K., and D. Duke (2011) An Archaeologically Validated Protocol for Computing Obsidian Hydration Rates from Laboratory Data. *Journal of Archaeological Science* 38:1340-1345.

Rogers, A.K., and D. Duke (2014) Unreliability of the Induced Hydration Method with Abbreviated Hot-Soak Protocols. *Journal of Archaeological Science* 52:428-435.

Stevenson, C.M., J.J. Mazer, and B.E. Scheetz (1998) Laboratory Obsidian Hydration Rates: Theory, Method, and Application. In M. S. Shackley (Ed.) *Archaeological Obsidian Studies: Method and Theory. Advances in Archaeological and Museum Science*, Vol. 3, pp.181-204. Plenum Press, New York.

Stevenson, C.M., and S.W. Novak (2011) Obsidian Hydration Dating by Infrared Spectroscopy: Method and Calibration. *Journal of Archaeological Science* 38:1716-1726.

Stevenson, C.M., and A.K. Rogers (2014) Transient and Equilibrium Solubility of Water in Rhyolitic Glass: Implications for Hydration Rate Development at Elevated Temperature. *Journal of Archaeological Science* 45:15-19.

NEW ANALYSES OF LATE HOLOCENE OBSIDIANS FROM SOUTHERN PATAGONIA (SANTA CRUZ PROVINCE, ARGENTINA)

Hugo G. Nami[1 2], Martin Giesso[3], Alicia Castro[4], Michael D. Glascock[5]

[1]CONICET- IGEBA, Dpto. Ciencias Geológicas, FCEN, UBA. Ciudad Universitaria, Pab.II, (C1428EHA), CABA.
[2]Associate Researcher, National Museum of Natural History, Smithsonian Institution, Washington D.C. E-mail: hgnami@fulbrightmail.org
[3] Department of Anthropology, Northeastern Illinois University, Chicago, Il 60625
[4] División Arqueología, Museo de La Plata, Universidad Nacional de La Plata, Argentina.
[5] Archaeometry Laboratory, University of Missouri Research Reactor, Columbia, Missouri, 65211

Introduction

Patagonia is a region of ~1 million square km located south of the Colorado and Bio-Bio rivers in Argentina and Chile respectively. The Santa Cruz province, in Argentina's southernmost continental portion is a territory where obsidian was a valuable tool-making resource for hunter-gatherers who inhabited the region during the Holocene. With the use of different analytical methods, regional obsidian sourcing has been a topic of interest for many years. The methods have allowed identification of the origin of most archaeological volcanic glasses used in the region since the late 1990s (Belardi et al. 2006; Bellelli and Pereyra 2002; Espinosa and Goñi 1999; Fernandez et al. 2015; Stern 1999; Stern and Franco 2000; Stern et al. 2000, Vásquez et al. 2001). The aim of this current project was to build on these previous investigations. As such, we analyzed a number of archaeological samples collected along the North Central coast and SE Santa Cruz Province of the Argentine Republic (Fig. 1). Samples from sources located in the area were collected as well. The samples reported here provide an extension of the Pampa del Asador source, and evidence of two new sources from as of yet unknown locations.

Materials

Forty one obsidian samples from the North Central Coast (NCC) were recovered in a systematic survey performed between Puerto Deseado and Bahia Laura, Deseado Department. During this endeavor, sampling units 1 km long were used along the Atlantic shoreline. The survey was made following the maximum tide line where vegetation begins and 100 meters inward of the continent. This

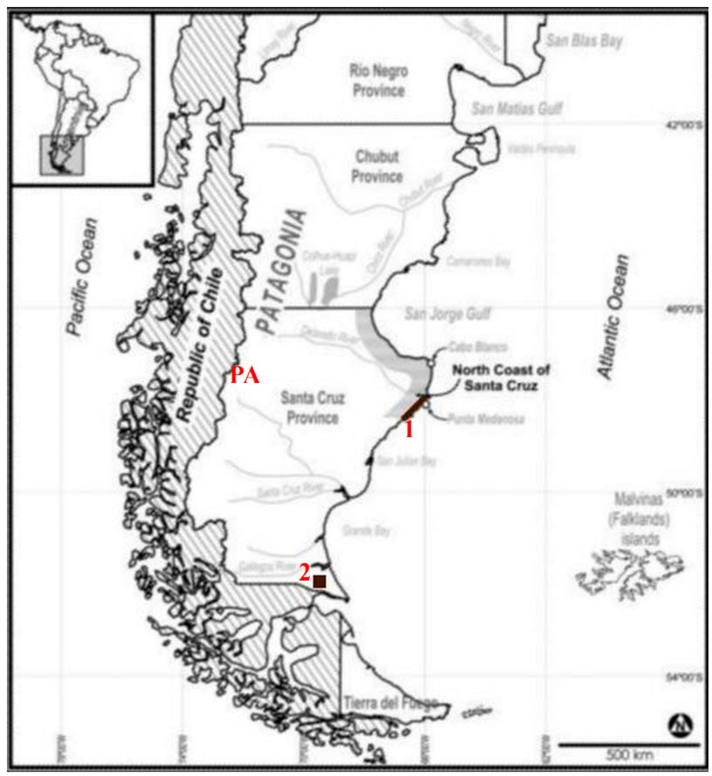

Figure 1. Map of Patagonia with the location of the sites mentioned in the text. PA: Pampa del Asador source, 1: North central coast, 2: Aristizabal Cave and Alero del Valle rockshelter.

located archaeological shell middens, as well as secondary sources (*sensu* Luedke 1979) of diverse rocks. Concentrations of pebbles and cobbles were found on the beach and paleo-beaches, but also on the eolian deposits along the strip of land bordering the coast. Remarkably, among these were pebbles of obsidian whose cortex indicates that they were rolled by the sea (Fig. 2). Radiocarbon dates obtained in the middens from the NCC of Santa Cruz indicate that the archaeological obsidian was used by Late Holocene hunter-gatherers.

The sample from southern Santa Cruz includes 14 specimens from Alero del Valle (AV), and two from Aristizábal Cave (AC). The former is a small rockshelter ~9 m wide by 1.5 m deep formed on a cliff on a terrace of the Chico River about 5 km north of the Markatch Aike ranch. The excavation revealed four natural strata. The artifacts analyzed were excavated from level III, corresponding to late Holocene hunter-gatherers dated between ~1.0 -3.0 kybp. Three carbon samples from these levels yielded uncalibrated radiocarbon dates of 1030 ± 60 (Beta-103247), 2520 ± 80 (Beta-103246), and 2870 ± 70 (Beta-115678) years b.p. AC (51º 54.75'S, 69º 44.76'W) is ~10 km west of AV at the top of Felton Hill, one of the highest elevations in the area. It is 16 m long and 8 m wide at the mouth, making it one of the largest caves known in the Pali Aike region. Excavation revealed five natural stratigraphic layers. Archaeological remains in layer IV indicate that this cave was used by late Holocene hunter-gatherers.

Located in the northwest of Santa Cruz, the most important known obsidian source in the province is Pampa del Asador (PA, Stern 1999). Our results are consistent with the fact that Pampa del Asador is the only obsidian type present on the northern Santa Cruz coast as along as the southern Chubut coast. To compare with the sample reported in this paper, and using the same methodology, we analyzed some specimens from this source.

Figure 2. Examples of obsidian nodules found in the northeast coast of Santa Cruz province showing smooth and well-rounded surfaces eroded by the sea.

Methods, Analysis and Results

The studied sample (n = 81) comes from the following locations: NCC (n = 41); AV (n = 14), AC (n = 2), and PA (n = 24) (See Table 1). All obsidians were analyzed by X-ray fluorescence (XRF) and 32 by neutron activation analysis (NAA) at the University of Missouri Research Reactor (MURR). XRF was employed on the totality of the sample, while NAA was used for the specimens coming from PA and from sites in the north central coast. XRF was performed using a hand-held spectrometer made by Bruker Corporation (Tracer III-V, serial number K0557). The apparatus is equipped with an air-cooled, rhodium target anode and 140 micron Be window. X-rays were measured by a thermoelectrically-cooled Si-PIN diode detector. The detector has a nominal resolution of 180 eV when measuring the 6.4 keV peak from iron. For the analyses reported here, the X-ray tube was operated at 40 kV

Table 1. XRF Results for Santa Cruz

ANID	Compositional Group	K	Ti	Mn	Fe	Zn	Ga	Rb	Sr	Y	Zr	Nb	Th	Sample Type	Site Name	Source Name
PAC001	PDA-1	38925.5	672.3	503.9	10014.2	89.7	21.9	186.4	30.5	32.9	136.8	26.7	19.8	source	Pampa del Asador	Pampa del Asador-1
PAC002	PDA-1	36714.9	776.9	274.9	10441.7	81.3	20.6	198.1	32.8	31.5	139.4	23.4	21.0	source	Pampa del Asador	Pampa del Asador-1
PAC003	PDA-1	37663.6	688.7	490.7	10467.8	99.3	20.8	211.3	34.6	33.1	145.3	24.0	16.3	source	Pampa del Asador	Pampa del Asador-1
SCAV01	SCAV-1	36139.4	517.6	329.1	19617.5	412.4	38.5	353.7	0.0	137.6	806.1	200.1	43.0	artifact	Alero del Valle	Alero del Valle-1
SCAV02	SCAV-1	36660.2	522.2	278.4	14992.2	290.6	36.3	304.2	0.0	123.4	755.9	191.7	42.6	artifact	Alero del Valle	Alero del Valle-1
SCAV03	SCAV-1	35003.4	599.4	377.8	16968.7	345.5	40.0	332.8	2.0	121.9	792.6	187.5	36.8	artifact	Alero del Valle	Alero del Valle-1
SCAV04	SCAV-1	35257.4	698.6	383.6	25320.9	614.1	36.9	377.2	0.0	144.5	858.1	207.5	43.3	artifact	Alero del Valle	Alero del Valle-1
SCAV05	SCAV-1	35697.8	720.6	534.9	24329.5	548.6	42.2	420.8	3.6	150.0	935.6	222.5	47.3	artifact	Alero del Valle	Alero del Valle-1
SCAV06-11	SCAV-1	33832.6	696.5	383.0	23862.0	435.9	43.0	340.1	1.7	123.6	736.1	186.0	42.1	artifact	Alero del Valle	Alero del Valle-1
SCAV12	SCAV-1	35246.8	678.1	342.8	18901.5	315.5	41.0	368.8	2.8	140.6	895.4	221.7	40.3	artifact	Alero del Valle	Alero del Valle-1
SCAV13	SCAV-1	34997.6	730.0	430.1	19048.3	336.5	33.1	334.6	2.5	127.9	808.2	200.7	37.1	artifact	Alero del Valle	Alero del Valle-1
SCAV14-15	SCAV-1	33821.6	537.4	274.9	18962.6	339.8	30.9	314.7	0.0	121.6	700.1	166.3	33.6	artifact	Alero del Valle	Alero del Valle-1
SCAV16	SCAV-1	36926.7	579.2	281.9	17276.7	284.5	38.2	337.2	0.7	144.4	867.2	213.4	41.5	artifact	Alero del Valle	Alero del Valle-1
SCAV17	SCAV-2	38366.4	541.3	227.3	8568.5	81.1	18.7	181.9	22.2	36.0	142.4	35.4	19.9	artifact	Alero del Valle	Alero del Valle-2
SCAV18	SCAV-2	34083.0	484.9	210.2	10609.6	102.8	19.4	195.3	23.5	37.1	140.5	35.4	19.9	artifact	Alero del Valle	Alero del Valle-2
SCAV19	SCAV-1	36271.8	361.8	412.4	19401.9	347.8	43.3	350.2	1.4	129.4	806.8	194.9	41.8	artifact	Alero del Valle	Alero del Valle-1
SCAV20	SCAV-1	35752.6	485.3	476.4	21033.4	379.7	44.3	372.8	0.0	135.8	837.2	194.7	43.4	artifact	Alero del Valle	Alero del Valle-1
SCCA01	SCCA-1	35856.8	486.2	461.3	13191.5	119.0	22.9	222.8	35.9	32.9	138.2	25.0	20.8	artifact	Cueva Ariztizabal	Cueva Ariztizabal
SCCA02	SCCA-1	36020.5	517.9	433.1	15138.7	134.8	24.2	246.5	41.6	42.3	155.7	24.2	25.3	artifact	Cueva Ariztizabal	Cueva Ariztizabal
SCPA01	PDA-1	36028.5	637.1	277.6	10048.0	60.3	23.0	189.3	29.1	33.8	150.5	26.0	23.7	source	Pampa del Asador	Pampa del Asador-1
SCPA02	PDA-1	37971.9	511.9	392.5	10458.4	68.5	19.6	193.4	32.2	30.0	128.6	20.6	13.7	source	Pampa del Asador	Pampa del Asador-1
SCPA03	PDA-2	35232.0	652.5	316.2	9474.4	81.8	19.7	225.3	0.4	49.2	138.0	26.5	20.5	source	Pampa del Asador	Pampa del Asador-2
SCPA04	PDA-1	37249.7	695.9	338.4	11086.2	54.2	18.7	204.2	33.5	34.6	144.8	24.6	17.6	source	Pampa del Asador	Pampa del Asador-1
SCPA05	PDA-3	35540.0	715.5	413.6	7158.6	45.5	15.7	145.3	35.5	12.4	141.0	26.2	19.2	source	Pampa del Asador	OUTLIER

ANID	Compositional Group	K	Ti	Mn	Fe	Zn	Ga	Rb	Sr	Y	Zr	Nb	Th	Sample Type	Site Name	Source Name
SCPA06	PDA-2	36371.2	682.9	536.6	13989.7	85.0	19.2	181.0	63.2	32.0	284.4	30.3	19.2	source	Pampa del Asador	Pampa del Asador-3
SCPA07	PDA-3	35024.8	714.9	368.2	8181.9	67.1	15.0	206.1	0.0	37.2	131.0	29.2	16.8	source	Pampa del Asador	Pampa del Asador-2
SCPA08	PDA-1	35363.0	623.6	400.0	14313.5	51.8	17.6	186.4	58.3	30.8	283.4	33.3	16.0	source	Pampa del Asador	Pampa del Asador-3
SCPA09	PDA-2	35361.4	626.1	268.6	10263.9	87.6	17.6	193.5	29.9	23.5	120.3	22.3	21.3	source	Pampa del Asador	Pampa del Asador-1
SCPA10	PDA-1	36350.4	841.8	312.8	10146.9	101.9	24.7	242.2	2.7	41.4	152.4	30.0	17.4	source	Pampa del Asador	Pampa del Asador-2
SCPA11	PDA-3	37444.2	642.4	387.8	10860.0	79.1	23.3	201.2	34.3	37.9	147.4	24.4	18.4	source	Pampa del Asador	Pampa del Asador-1
SCPA12	PDA-2	35260.5	995.4	504.6	12680.6	87.9	20.2	191.4	44.0	32.6	250.7	31.7	21.7	source	Pampa del Asador	Pampa del Asador-3
SCPA13	PDA-1	36264.9	787.9	280.6	10137.7	115.4	21.7	258.5	0.4	54.5	159.3	35.2	17.7	source	Pampa del Asador	Pampa del Asador-2
SCPA14	PDA-1	36579.5	767.1	370.1	10259.0	78.5	17.8	197.1	35.7	25.6	144.2	28.7	16.5	source	Pampa del Asador	Pampa del Asador-1
SCPA15	PDA-3	36793.3	782.2	358.4	10839.3	99.3	17.5	197.5	36.3	36.2	143.4	25.9	18.8	source	Pampa del Asador	Pampa del Asador-1
SCPA16	PDA-1	36148.3	866.7	427.4	14038.3	88.8	21.1	180.9	64.5	30.2	293.8	29.6	21.0	source	Pampa del Asador	Pampa del Asador-3
SCPA17	PDA-2	35382.5	627.1	176.6	10129.8	111.2	19.0	173.5	27.6	25.4	117.7	20.1	15.7	source	Pampa del Asador	Pampa del Asador-1
SCPA18	PDA-2	37258.6	578.1	233.8	10765.4	77.8	19.4	244.3	3.7	43.1	158.2	30.8	17.4	source	Pampa del Asador	Pampa del Asador-2
SCPA19	PDA-2	35906.5	519.8	266.8	10928.9	94.5	23.7	226.5	0.7	39.3	148.1	26.3	17.7	source	Pampa del Asador	Pampa del Asador-2
SCPA20	PDA-3	36228.4	463.3	289.2	11646.5	100.5	22.0	265.2	1.8	42.3	162.2	31.4	21.4	source	Pampa del Asador	Pampa del Asador-2
SCPA21	PDA-2	34956.4	686.9	346.2	14799.5	83.1	22.4	191.5	63.7	31.3	309.5	33.5	20.2	source	Pampa del Asador	Pamap del Asador-3
SCPM01	PDA-1	38855.3	789.8	416.5	9965.5	105.8	22.5	230.1	2.9	46.6	149.6	31.0	22.7	source	Punta Medanosa	Pampa del Asador-2
SCPM02	PDA-2	37360.4	888.7	298.1	8927.9	78.8	20.3	186.6	27.7	26.3	128.6	26.5	17.3	source	Punta Medanosa	Pampa del Asador-1
SCPM03	PDA-1	37783.0	692.3	338.1	8115.2	92.4	18.6	220.9	0.5	41.1	137.0	28.7	19.6	source	Punta Medanosa	Pampa del Asador-2
SCPM05	PDA-1	38530.0	770.3	407.6	10376.3	81.2	20.3	202.5	31.5	32.1	146.8	24.5	20.0	source	Punta Medanosa	Pampa del Asador-1
SCPM06	PDA-1	37770.4	763.0	372.3	10614.2	59.0	17.4	204.8	32.2	30.3	139.2	22.8	18.5	source	Punta Medanosa	Pampa del Asador-1
SCPM08	PDA-1	36108.6	600.4	228.3	10538.3	73.8	20.0	200.1	31.9	28.5	142.1	28.2	15.0	source	Punta Medanosa	Pampa del Asador-1
SCPM09	PDA-1	37300.4	654.5	283.6	10949.5	76.5	21.7	210.3	28.4	32.3	139.4	24.8	20.7	source	Punta Medanosa	Pampa del Asador-1
SCPM10	PDA-1	36117.4	845.3	424.8	10426.0	85.2	23.9	193.3	28.5	30.5	131.9	22.7	18.4	source	Punta Medanosa	Pampa del Asador-1
SCPM11	PDA-1	36971.6	642.7	377.1	10421.4	64.7	20.9	199.3	30.5	28.7	140.5	24.7	18.4	source	Punta Medanosa	Pampa del Asador-1

ANID	Compositional Group	K	Ti	Mn	Fe	Zn	Ga	Rb	Sr	Y	Zr	Nb	Th	Sample Type	Site Name	Source Name
SCPM12	PDA-1	36782.4	583.6	322.0	10745.5	87.8	19.0	207.6	32.0	31.1	145.6	23.0	23.0	source	Punta Medanosa	Pampa del Asador-1
SCPM13	PDA-1	36346.5	680.2	363.4	9806.9	67.3	22.0	188.9	30.1	32.8	126.7	21.7	15.7	source	Punta Medanosa	Pampa del Asador-1
SCPM14	PDA-2	36397.9	586.2	306.6	10083.0	84.4	15.7	235.5	3.0	45.1	161.4	30.8	18.0	source	Punta Medanosa	Pampa del Asador-2
SCPM15	PDA-1	38622.4	556.2	291.7	10709.1	72.5	16.9	200.1	33.6	34.0	145.1	25.5	21.6	source	Punta Medanosa	Pampa del Asador-1
SCPM16	PDA-3	36362.8	705.5	497.5	13845.1	44.7	21.8	181.0	67.3	23.0	269.2	32.1	20.5	source	Punta Medanosa	Pampa del Asador-3
SCPM17	PDA-1	37678.0	518.2	413.8	10669.5	56.9	20.5	196.2	32.9	33.9	144.5	22.6	14.8	source	Punta Medanosa	Pampa del Asador-1
SCPM18	PDA-3	36616.7	768.0	479.9	14311.1	70.3	16.6	175.6	61.3	30.0	268.1	30.1	19.4	source	Punta Medanosa	Pampa del Asador-3
SCPM19	PDA-1	36300.3	683.3	294.9	10914.1	89.0	20.3	220.7	30.6	32.9	144.8	25.5	23.5	source	Punta Medanosa	Pampa del Asador-1
SCPM20	PDA-2	37165.4	734.1	335.9	9310.4	78.1	18.1	213.5	3.4	39.9	143.6	29.0	16.4	source	Punta Medanosa	Pampa del Asador-2
SCPM21	PDA-2	37299.0	653.6	435.5	10013.3	73.4	23.4	236.3	3.6	48.0	148.1	29.2	22.7	source	Punta Medanosa	Pampa del Asador-2
SCPM22	PDA-1	36582.6	795.9	422.1	11396.5	101.8	20.6	213.4	34.1	39.8	151.0	24.3	21.1	source	Punta Medanosa	Pampa del Asador-1
SCPM23	PDA-1	37441.5	556.1	412.6	9904.8	70.3	19.1	201.3	35.9	28.1	138.6	24.9	18.5	source	Punta Medanosa	Pampa del Asador-1
SCPM24	PDA-1	36671.9	752.1	458.5	11850.3	58.8	18.8	209.9	30.3	32.2	158.5	25.2	21.5	source	Punta Medanosa	Pampa del Asador-1
SCPM25	PDA-2	37063.2	638.3	260.5	8803.1	86.1	22.7	215.3	3.7	40.8	145.5	25.2	14.7	source	Punta Medanosa	Pampa del Asador-2
SCPM26	PDA-2	37512.6	685.8	321.2	9975.3	77.2	21.1	215.6	2.0	42.4	150.9	28.3	19.3	source	Punta Medanosa	Pampa del Asador-2
SCPM27	PDA-1	37064.4	772.6	361.3	10719.6	71.3	21.3	195.1	34.7	32.7	145.7	24.5	21.3	source	Punta Medanosa	Pampa del Asador-1
SCPM28	PDA-2	37146.0	604.9	389.2	10215.0	90.5	18.9	239.6	2.6	43.8	154.4	28.5	21.7	source	Punta Medanosa	Pampa del Asador-2
SCPM29	PDA-2	36788.4	627.4	474.4	9568.2	72.2	19.6	227.3	2.6	41.7	148.2	25.7	19.4	source	Punta Medanosa	Pampa del Asador-2
SCPM30	PDA-1	37337.2	724.3	309.3	10430.7	68.5	26.9	203.3	32.9	32.1	145.9	26.1	23.9	source	Punta Medanosa	Pampa del Asador-1
SCPM31	PDA-1	37489.2	678.0	336.4	10896.4	62.9	22.2	208.9	34.0	31.0	148.6	25.1	19.2	source	Punta Medanosa	Pampa del Asador-1
SCPM32	PDA-1	36452.7	679.7	406.8	10800.0	80.3	16.2	200.7	34.3	31.8	145.9	26.6	19.5	source	Punta Medanosa	Pampa del Asador-1
SCPM33	PDA-2	36616.6	751.8	229.7	8645.1	60.4	26.8	238.3	0.6	42.8	144.8	34.5	21.6	source	Punta Medanosa	Pampa del Asador-2
SCPM34	PDA-1	35921.3	926.6	391.7	11013.5	84.5	20.6	205.9	35.2	36.5	143.5	27.9	19.9	source	Punta Medanosa	Pampa del Asador-1
SCPM35	PDA-1	37892.2	671.1	414.4	10200.2	101.5	21.3	176.0	27.3	30.7	125.5	21.4	18.5	source	Punta Medanosa	Pampa del Asador-1
SCPM36	PDA-1	36934.2	679.0	355.8	10818.5	63.1	23.3	201.5	33.6	40.0	158.5	25.6	20.2	source	Punta Medanosa	Pampa del Asador-1

ANID	Compositional Group	K	Ti	Mn	Fe	Zn	Ga	Rb	Sr	Y	Zr	Nb	Th	Sample Type	Site Name	Source Name
SCPM37	PDA-2	36362.9	622.6	366.8	9376.3	60.3	27.1	241.9	0.0	47.8	148.7	32.3	22.1	source	Punta Medanosa	Pampa del Asador-2
SCPM38	PDA-1	36412.6	774.9	483.3	9971.1	59.5	19.8	203.9	30.0	29.4	139.5	28.5	22.1	source	Punta Medanosa	Pampa del Asador-1
SCPM39	PDA-1	36335.3	869.7	436.0	10205.0	79.7	21.0	193.1	34.4	31.4	149.8	24.1	20.0	source	Punta Medanosa	Pampa del Asador-1
SCPM40	PDA-1	36986.7	693.6	467.1	10298.8	62.9	20.5	211.4	33.8	32.3	150.2	28.8	24.8	source	Punta Medanosa	Pampa del Asador-1
SCPM41	PDA-2	36741.4	519.3	325.7	9357.1	107.8	24.4	227.9	2.1	41.9	155.0	31.5	19.3	source	Punta Medanosa	Pampa del Asador-2
SCPM42	PDA-1	36711.4	621.4	362.0	10810.7	81.8	17.2	201.7	34.4	34.0	144.4	27.4	18.5	source	Punta Medanosa	Pampa del Asador-1
SCPM43	PDA-1	36446.5	652.4	311.1	10959.7	62.1	11.0	209.1	35.8	29.1	134.0	22.1	18.1	source	Punta Medanosa	Pampa del Asador-1

Table 2. NAA Results for Santa Cruz

ANID	Source Name	La	Lu	Nd	Sm	U	Yb	Ce	Co	Cs	Eu	Fe	Hf	Rb	Sb	Sc	Sr
SCPA01	Pampa del Asador-1	38.9754	0.5242	30.8480	6.7846	5.5674	3.3452	76.1854	0.2425	10.4550	0.2736	9867.7	5.4611	199.71	0.3283	7.2558	0.00
SCPA02	Pampa del Asador-1	39.3888	0.6315	30.2806	6.7731	6.1380	3.4283	77.0908	0.2823	10.5093	0.2784	10258.8	5.6319	201.81	0.3193	7.4161	0.00
SCPA03	Pampa del Asador-1	23.0629	0.8135	26.9336	7.9959	7.0285	4.6693	54.7534	0.2424	13.0272	0.0915	9209.0	6.2888	238.98	0.2939	9.5950	0.00
SCPA04	Pampa del Asador-1	38.6139	0.5143	30.1792	6.7728	6.4424	3.3825	75.7471	0.2491	10.3520	0.2734	9867.3	5.4197	200.15	0.3493	7.2470	43.61
SCPA06	Pampa del Asador-2	43.7467	0.5949	30.2429	6.2225	6.8291	3.1644	81.3558	0.6845	5.8331	0.7161	13356.9	7.7483	174.45	0.2628	4.9055	73.70
SCPA08	Pampa del Asador-2	44.1712	0.6012	32.0856	6.2023	6.5653	3.1305	81.7512	0.4824	5.8117	0.7143	12945.7	7.6354	174.98	0.2738	4.8828	65.26
SCPA10	Pampa del Asador-2	27.9944	0.6441	29.0919	7.7700	6.1335	4.2580	63.8701	0.0577	11.7089	0.1162	9066.2	6.1340	223.51	0.2613	9.6737	0.00
SCPA11	Pampa del Asador-1	38.1530	0.5120	28.4666	6.7195	6.2345	3.4202	74.4935	0.2256	10.2239	0.2575	9622.3	5.5245	201.36	0.3318	7.1208	41.67
SCPA12	Pampa del Asador-1	42.6818	0.5155	29.7491	5.9652	7.5047	3.0821	81.1185	0.3643	5.9886	0.6165	11818.1	7.1916	181.83	0.2435	4.7537	24.96
SCPA13	Pampa del Asador-2	22.8396	0.7349	27.5919	8.0069	7.7811	4.7351	53.9253	0.0623	12.8514	0.0918	8655.3	6.1477	241.61	0.3144	9.3380	0.00
SCPA14	Pampa del Asador-1	38.2955	0.5351	28.4103	6.6809	5.9100	3.3038	75.0155	0.2501	10.3159	0.2775	9775.9	5.4964	199.05	0.3128	7.1875	27.60
SCPA15	Pampa del Asador-1	38.3433	0.5149	29.9071	6.7337	5.9465	3.2687	76.0945	0.2286	10.3346	0.2700	9829.2	5.3859	199.76	0.3183	7.2410	31.74
SCPA16	Pampa del Asador-3	44.1448	0.5283	30.9620	6.2563	6.7424	3.1127	82.7756	0.4732	5.7793	0.7351	12918.8	7.6713	176.64	0.2394	4.8973	68.52
SCPM01	Pampa del Asador-2	29.2736	0.6958	39.9981	9.6151	7.5972	4.7527	66.7715	0.0579	12.2987	0.1126	9569.6	6.4065	229.90	0.2541	10.2147	0.00
SCPM02	Pampa del Asador-1	39.0725	0.5551	24.4990	8.2231	7.0056	3.5555	77.8402	0.2554	10.7076	0.2802	10152.8	5.4871	204.00	0.3093	7.5107	22.25
SCPM03	Pampa del Asador-2	23.3143	0.7740	25.8154	9.3109	7.6164	4.6181	56.2280	0.0411	13.3752	0.0844	8968.3	6.4564	244.42	0.2912	9.7078	0.00
SCPM05	Pampa del Asador-1	38.5702	0.5484	28.1851	8.0421	6.5393	3.3618	75.9376	0.2343	10.5024	0.2732	9922.4	5.3552	201.97	0.3099	7.2763	20.03
SCPM06	Pampa del Asador-1	38.9133	0.5654	26.3231	8.0676	7.6246	3.5487	76.8445	0.2400	10.5400	0.2805	10014.0	6.0786	202.38	0.3124	7.3802	35.40
SCPM08	Pampa del Asador-1	37.7025	0.5422	32.6496	7.7941	6.8570	3.1116	73.8475	0.2301	10.2631	0.2673	9637.8	5.4517	196.26	0.3166	7.1156	17.88
SCPM09	Pampa del Asador-1	38.0867	0.5643	27.2093	7.8876	6.8772	3.1832	74.9386	0.2279	10.3677	0.2715	9736.8	5.6127	200.41	0.3174	7.1915	25.24
SCPM10	Pampa del Asador-1	38.3841	0.6077	30.0916	7.9773	7.1017	3.2325	75.9857	0.2311	10.5762	0.2753	9924.7	5.4932	202.14	0.3147	7.3179	17.17
SCPM11	Pampa del Asador-1	38.1229	0.5655	30.4194	7.9891	7.0050	3.2135	76.3776	0.2302	10.5634	0.2694	9910.1	5.5573	203.03	0.3109	7.3053	26.19
SCPM12	Pampa del Asador-1	38.5882	0.5706	27.1248	7.9320	7.0408	3.2341	76.0036	0.2391	10.5217	0.2720	9890.8	5.5689	201.70	0.3406	7.3308	26.73
SCPM13	Pampa del Asador-1	39.3433	0.5812	31.3790	8.0646	7.2648	3.3901	77.6597	0.2511	10.6992	0.2784	10031.3	5.7348	200.96	0.3201	7.4385	37.25
SCPM14	Pampa del Asador-2	28.9675	0.6890	28.7009	9.3567	7.5991	4.0843	64.9954	0.0624	12.0281	0.1239	9309.3	6.2754	226.02	0.2311	9.9832	0.00
SCPM15	Pampa del Asador-1	38.7632	0.5700	27.0169	7.9603	7.5029	3.7408	76.9318	0.2755	10.4821	0.2738	10081.6	5.5001	201.51	0.3084	7.3819	26.73
SCPM16	Pampa del Asador-3	44.1749	0.5305	33.0233	7.2894	7.5838	3.0324	81.7702	0.4914	5.7740	0.7188	13112.2	7.7059	174.12	0.2523	4.8968	58.12
SCPM17	Pampa del Asador-1	38.7260	0.5662	30.8041	7.9992	7.0230	3.2491	76.3119	0.2391	10.5366	0.2781	9918.6	5.6197	200.44	0.3123	7.3424	12.93
SCPM18	Pampa del Asador-3	42.5377	0.5669	29.9240	7.1088	7.0461	2.8950	80.2286	0.4582	5.7392	0.6929	12589.1	7.5117	172.93	0.2160	4.7979	68.54
SCPM19	Pampa del Asador-1	39.3295	0.5834	30.8912	8.0824	7.1813	3.3111	76.8732	0.2313	10.4668	0.2757	9972.9	5.4319	199.48	0.3098	7.3728	28.14
SCPM20	Pampa del Asador-2	28.5391	0.7429	32.0780	9.3620	7.5244	4.5918	64.4797	0.0647	11.9871	0.1135	9184.8	6.2119	224.48	0.2329	9.8552	0.00
SCPM21	Pampa del Asador-2	28.5213	0.7173	27.4356	9.3127	7.3164	4.0897	64.3036	0.0549	11.9290	0.1191	9152.7	6.1603	222.92	0.2390	9.7739	0.00

Table 2. NAA Results for Santa Cruz (continued)

ANID	Source Name	Ta	Tb	Th	Zn	Zr	Br	Al	Ba	Cl	Dy	K	Mn	Na
SCPA01	Pampa del Asador-1	2.0856	0.9916	18.4604	67.32	153.71	2.091	68883.2	246.00	506.5	6.3808	39774.2	275.38	28790.0
SCPA02	Pampa del Asador-1	2.1132	0.9827	18.6455	71.10	170.12	2.222	74041.8	279.40	510.9	6.4023	40842.2	287.36	29297.2
SCPA03	Pampa del Asador-1	2.5597	1.4396	19.2048	89.23	149.03	1.954	67803.6	22.80	444.6	10.1688	40374.4	237.34	29460.7
SCPA04	Pampa del Asador-1	2.0374	0.9793	18.3670	68.58	159.40	1.959	71335.9	262.00	502.2	6.4200	41758.9	283.07	29108.5
SCPA06	Pampa del Asador-2	2.3797	0.8101	20.7581	62.22	317.23	2.847	72842.2	559.80	612.3	5.2645	39097.2	390.78	33778.0
SCPA08	Pampa del Asador-2	2.3970	0.8130	20.7375	65.28	308.95	3.078	73626.4	568.80	593.3	5.1069	41470.3	390.85	33476.4
SCPA10	Pampa del Asador-2	2.3322	1.2455	18.4157	82.49	186.75	1.614	69978.0	0.00	446.1	9.3777	41190.0	241.34	29658.0
SCPA11	Pampa del Asador-1	2.0222	0.9635	18.0948	67.78	155.76	2.490	70129.5	262.60	407.9	6.4807	42974.7	287.20	29870.7
SCPA12	Pampa del Asador-1	2.4702	0.8394	21.3119	60.81	270.22	3.445	72251.3	529.30	544.2	5.2732	41068.4	378.60	34134.6
SCPA13	Pampa del Asador-2	2.5651	1.4042	18.9593	88.51	141.49	1.573	70867.1	0.00	515.0	9.8362	41727.6	219.34	29552.0
SCPA14	Pampa del Asador-1	2.0535	1.0895	18.1563	67.44	163.50	2.440	67603.8	251.10	515.2	6.3018	42257.5	278.88	29002.7
SCPA15	Pampa del Asador-1	2.0462	1.0070	18.2547	67.31	176.34	2.687	71773.2	256.90	464.6	6.0564	42797.5	282.89	29708.2
SCPA16	Pampa del Asador-3	2.3533	0.8367	20.7488	62.92	302.28	2.297	70500.9	564.40	517.7	5.4186	39304.2	390.15	33898.5
SCPM01	Pampa del Asador-2	2.4250	1.3603	19.2156	88.05	177.30	1.776	68225.6	0.00	451.4	8.3408	39471.3	237.77	29098.1
SCPM02	Pampa del Asador-1	2.1178	1.0805	18.8095	70.05	174.00	2.197	69098.1	274.70	148.5	6.8236	40784.3	283.45	29479.1
SCPM03	Pampa del Asador-2	2.6210	1.4381	19.5977	82.42	170.40	1.964	70112.5	0.00	480.0	9.1220	40674.1	216.16	29414.1
SCPM05	Pampa del Asador-1	2.0812	0.9794	18.4161	72.41	163.96	1.787	69768.1	292.70	503.2	6.7207	40890.2	281.75	29144.2
SCPM06	Pampa del Asador-1	2.0786	0.9915	18.7064	68.77	186.64	2.446	70106.6	249.10	533.0	6.6276	40099.5	282.34	29400.5
SCPM08	Pampa del Asador-1	2.0179	1.0580	18.0099	70.61	165.34	2.466	71665.7	266.80	482.6	6.0616	43674.1	283.81	29509.8
SCPM09	Pampa del Asador-1	2.0617	0.9721	18.1818	71.55	166.92	2.024	67160.4	294.20	486.3	6.7210	42741.0	281.89	29945.9
SCPM10	Pampa del Asador-1	2.0872	1.0068	18.5985	72.82	165.00	1.963	73898.9	283.40	513.9	5.8181	43129.5	282.32	29615.0
SCPM11	Pampa del Asador-1	2.0874	1.0142	18.5903	72.10	169.19	2.160	67686.1	232.80	532.2	6.9185	39630.9	280.38	29444.2
SCPM12	Pampa del Asador-1	2.0580	1.0420	18.3837	72.36	172.38	2.268	66641.2	245.20	539.0	7.1851	41294.3	282.07	29311.3
SCPM13	Pampa del Asador-1	2.0736	1.0352	18.6703	73.57	176.04	2.610	68016.1	245.30	506.0	6.2929	37106.3	277.93	29295.3
SCPM14	Pampa del Asador-2	2.3823	1.4270	18.6764	96.92	178.64	1.816	70304.1	0.00	472.3	8.9260	43273.0	241.34	29799.2
SCPM15	Pampa del Asador-1	2.0804	0.9766	18.5326	78.91	166.00	2.351	66991.0	274.60	516.4	6.4098	42044.7	279.76	27303.1
SCPM16	Pampa del Asador-3	2.3572	0.8407	20.5954	66.47	303.49	3.368	75297.3	611.80	570.2	5.2568	39264.7	392.43	33379.2
SCPM17	Pampa del Asador-1	2.0595	1.0674	18.4998	73.13	169.10	2.548	69376.1	279.20	452.7	6.5235	42390.0	279.54	29343.4
SCPM18	Pampa del Asador-3	2.3542	0.8151	20.3848	64.26	301.85	3.610	65464.8	591.20	549.9	5.9566	40688.5	384.20	33381.6
SCPM19	Pampa del Asador-1	2.0707	1.0388	18.4687	76.11	169.63	2.245	71991.3	284.80	493.0	6.1041	44493.9	282.99	29599.6
SCPM20	Pampa del Asador-2	2.3493	1.3690	18.6227	92.14	173.80	2.088	65470.4	62.50	285.7	9.4515	41467.3	239.84	29587.0
SCPM21	Pampa del Asador-2	2.3490	1.3056	18.6630	86.04	156.19	1.513	67415.2	0.00	437.7	9.3731	40799.3	239.73	29485.1

with a tube current of 17μA. The beam dimensions are about 2 x 3 mm. Measurement times were 180 seconds. The counting rate was approximately 1,200 counts per second for samples larger than the minimum recommended size. Smaller samples produced count rates as low as 300 counts per second. Peak deconvolution was accomplished using the Bruker spectral analysis package which enabled measurement of thirteen elements in most samples, including K, Ti, Mn, Fe, Zn, Ga, Rb, Sr, Y, Zr, Nb, Pb, and Th. The instrument was calibrated using compositional data from a series of well-characterized source samples in the MURR obsidian reference collection, including eleven Mesoamerican sources (El Chayal, Ixtepeque, San Martin Jilotepeque, Guadalupe Victoria, Pico de Orizaba, Otumba, Paredon, Sierra de Pachuca, Ucareo, Zaragoza, and Zacualtipan) and three Peruvian sources (Alca, Chivay, and Quispisisa). Consensus values for the obsidian calibration sources were previously determined at MURR (using both NAA and XRF) and other laboratories (XRF only). Concentration ranges for the reference samples span the range of probable concentrations for obsidian from different sources around the world.

NAA is a technique that analyzes a larger number of chemical elements (up to 32), it is more expensive and takes several weeks to collected the data. It is also destructive. NAA of obsidian at MURR consists of two neutron irradiations by neutrons followed by three measurements of the emitted gamma radiation. The first irradiation for five seconds was applied to samples weighing about 100 mg encapsulated in a polyethylene vial using a thermal neutron flux of $8x10^{13}$ n cm^{-2} s^{-1}. This short irradiation was followed a 25–minute decay and 12–minute count which allowed measurement of seven short-lived elements (i.e., Al, Ba, Cl, Dy, K, Mn, and Na). The second irradiation was applied to a bundle of obsidian samples and standards weighing between 50 and 250 mg which were encapsulated in high-purity quartz vials and subjected to a long irradiation of 70 hours using a thermal neutron flux of $5x10^{13}$ n cm^{-2} s^{-1}. The long irradiation was followed by two gamma-ray counts. The first count was performed between seven and eight days after the end of irradiation, using a sample changer to count each sample for 30 minutes, to detect seven medium-lived elements (i.e., Ba, La, Lu, Nd, Sm, U, and Yb). The second count was performed about four weeks after the end of irradiation, using the sample changer for three hours per sample, to detect fifteen long-lived elements (i.e., Ce, Co, Cs, Eu, Fe, Hf, Rb, Sb, Sc, Sr, Ta, Tb, Th, Zn, and Zr). When the long irradiation is performed, the barium concentration from measurement of the medium-lived isotope (i.e., ^{133}Ba) is normally superior and it is used in lieu of the value for Ba measured following the short-lived irradiation. The data from all three measurements were converted to concentrations by comparing the unknown

Locality/Site	Samples (n)	Provenance	Observations
NCC	28	PA 1	Analyzed by XRF and NAA
NCC	11	PA 2	Analyzed by XRF and NAA
NCC	2	PA 3	Analyzed by XRF and NAA. Characterized by very low Sr
AV	12	Unknown Source a	Characterized by high Zr
AV	2	Unknown Source b	
AC	2	Unknown Source c	

Table 3. Provenance and techniques applied.

samples to the count rates for standards counted with the samples. All concentration data were compiled into a spreadsheet.

The detailed results by elements and provenience are respectively depicted in Tables 1 and 2.

Of the 14 artifacts from Alero del Valle, 12 belong to one source and two to another (AV17 and 18). The two samples from Aristizábal Cave belong to a third unknown source. At the moment we cannot attribute these three unknown sources with the other Patagonian sources in the MURR database, but we can presume that Unknown Source b could potentially match Cordillera Baguales.

Of the known sources, there is a green striped type of obsidian named Cordillera Baguales, which is found in Lago Argentino, and in the Fell and Pali Aike caves, where it represents one-third to one-fifth of the total obsidian (Stern and Franco 2000). In other words, it was procured by peoples living to the east and south of the source, particularly along the Atlantic coast (Fig. 4). It is characterized by very small amounts of Sr in ppm, as Unknown Sources a and b.

Discussion and Conclusion

New data obtained for obsidian artifacts from diverse locales in Santa Cruz province, Argentina have been found to contain trace elements indicating diverse origins. Detailed XRF and NAA analyses show that the provenance of samples from NCC is the well-known source of PA, the obsidian source most often used in southern Argentine Patagonia. These artifacts have the fingerprints of the three sub sources differentiated by Stern (1999). Tools made using this natural glass are found at sites in the provinces of Chubut and Santa Cruz, in the cordillera, in the central sector and along the Atlantic coast (Belardi et al. 2006, Fernandez et al. 2015, Stern 1999, Castro Esnal et al. 2011). However, it is worth mentioning that obsidian pebbles collected at secondary sources in the North Central Coast of Santa Cruz also originated from the same primary source, and were displaced downstream from the Andes, under what are called the “Rodados Tehuelches” or “Patagónicos” and “Gravas Tehuelches” (i.e., Auer 1956, Fidalgo and Riggi 1965, Martínez and Kutschker 2011, Franco et al. 2017) which

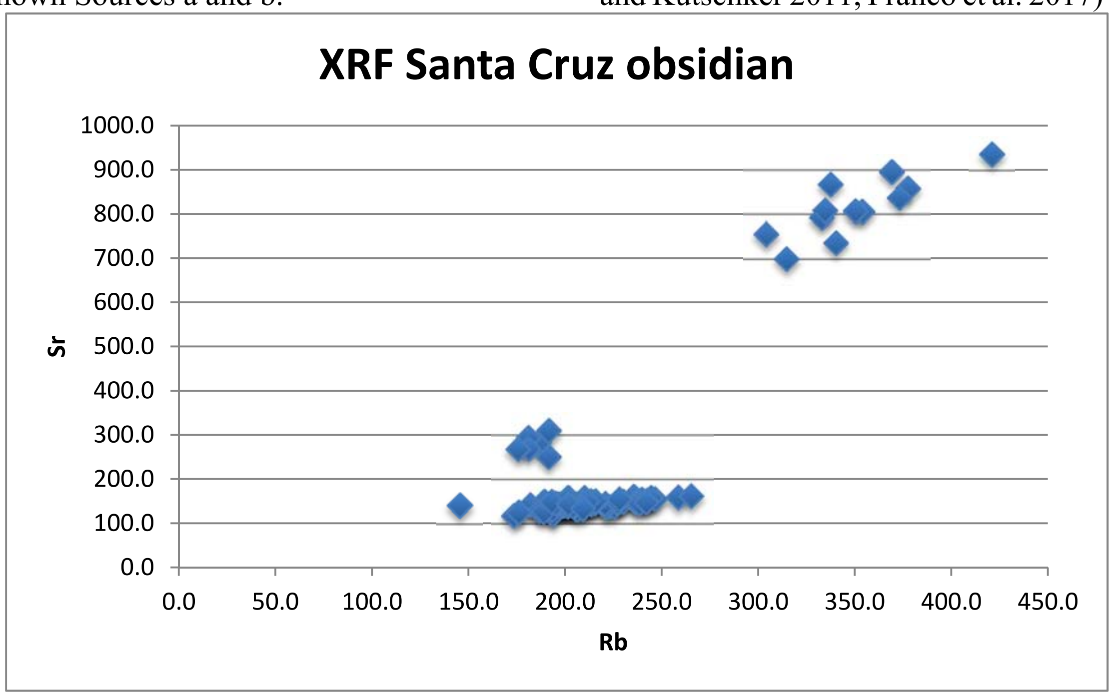

Figure 3. Rb-Sr Bivariate plot showing separation of three obsidian types.

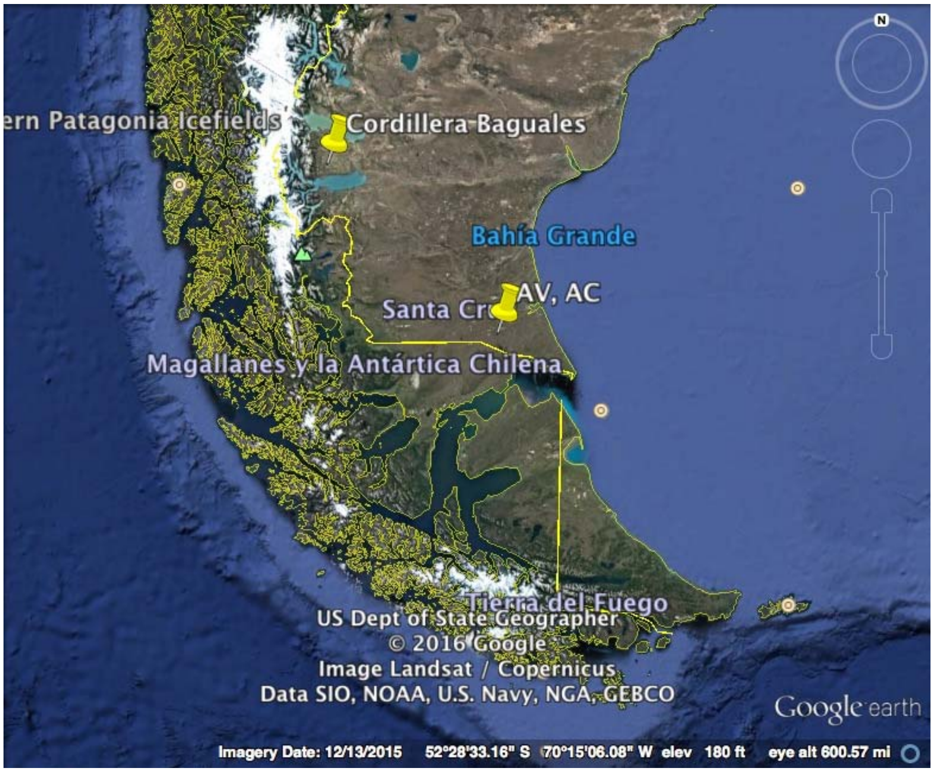

Figure 4. Cordillera Baguales and southernmost Patagonia sites.

are ubiquitous outcrops of pebbles and boulders with a diversity of rocks and varied lithology available depending on the area. Hence, due to the existence of obsidian nodules in the eolian deposits of the northeast coast of Santa Cruz, we suggest the possibility that obsidian nodules from PA were transported by some of the geological episodes that deposited the "rodados patagónicos" in the region (Martínez and Kutschker 2011). Similar PA obsidian was found in a secondary source 170km southeast of the main Pampa del Asador source (Franco et al 2017). Therefore, the secondary sources existing in the northeastern coast of Santa Cruz might contain some isolated PA obsidian nodules useful for stone tool manufacture, a fact that needs further investigation. In southeast Santa Cruz, obsidian was transported along the Chico River valley. Hence, some considerations may be made on the obsidian from unknown sources from AV and AC. Chaitén obsidian was found in archaeological sites of southern Santa Cruz. Cordillera Baguales, a green obsidian, is the most common obsidian in inland southern Patagonia. Among coastal sites, the also green Seno Otway obsidian is predominant. The only relationship we could establish is that Alero del Valle 1 has some resemblance to Cordillera Baguales, based on Mn, Rb, Sr, and particularly a very high Zr. Inhabitants from the Pali Aike region utilized obsidian from the main southern sources: Pampa del Asador, Cordillera Baguales and Seno Otway.

Acknowledgements.

We are deeply indebted to the University of Buenos Aires, University of La Plata, and the CONICET for their support, and to the National Science Foundation grant (1621158) to MURR.

References Cited

Ambrústolo, P., M. A. Zubimendi, and C. Stern (2012). Explotación de Obsidiana Negra en la Costa Norte de Santa Cruz (Patagonia argentina). *Revista Cazadores Recolectores del Cono Sur* 6: 77-86.

Auer, V. (1956) The Pleistocene of Fuego-Patagonia. Part I: The Ice and Interglacial Ages. *Annales Academiae Scientarum Fennicae* Series A, 3(45).

Belardi, J. B., P. Tiberi, C. Stein and A. Súnico (2006) Al Este del Cerro Pampa. Ampliación del Area de Disponibilidad de Obsidiana de la Pampa del Asador (Provincia de Santa Cruz). *Intersecciones en Antropología* 7: 27-36.

Bellelli, C. and F. X. Pereyra (2002) Analisis Geoquímicos de Obsidiana: Distribuciones, Fuentes y Artefactos Arqueológicos en el Noroeste del Chubut, Patagonia Argentina. *Werken* 3: 99-118.

Castro Esnal, A., C. Pérez De Micou, C. R. Stern (2011) Circulación de Obsidiana en Chubut, Patagonia Central, Argentina: Uso de las Materias Primas Extra-regionales como Indicadores de Movilidad e Interacción entre Grupos Cazadores Recolectores. *Revista do Museu de Arqueologia e Etnologia (São Paulo)* 21: 93-102.

Espinosa, S. and R. Goñi (1999) Viven: Una Fuente de Obsidiana en la Provincia de Santa Cruz. *Actas de las III Jornadas de Arqueología de la Patagonia: Soplando en el Viento*, J. Belardi, P. Fernández, R. Goñi, A. Guráieb and M. De Nigris (Eds.) pp. 177-188. INAPL, Buenos Aires.

Fernandez, M. V., C. Stern and P. Rodrigo (2015) Geochemical Analysis of Obsidian from Archaeological Sites in Northwestern Santa Cruz Province, Argentine Patagonia. *Quaternary International* 375: 44-54.

Fidalgo, F. and J. C. Riggi (1965) Rodados Patagónicos en la Meseta Guenguel y Alrededores (San Cruz). *Revista de la Asociación Geológica Argentina* XX (3): 273-325.

Luedtke, B. (1979) The Identification of Sources of Chert Artifacts. *American Antiquity* 44: 744–57.

Franco, N. V., G. A. Brook, N. A. Cirigliano, C. R. Stern and L. Ventrisano (2017) A New Distal Source of Pampa del Asador Type Black Obsidian and its Implications for Understanding Hunter-gatherer Behavior in Patagonia. *Journal of Archaeological Science: Reports* 12: 232-243.

Martinez, O. A. and M. Kutschker (2011) Los 'Rodados Patagónicos' (Patagonian Shingle Formation) of Eastern Patagonia: Environmental Conditions of Gravel Sedimentation. *Biological Journal of the Linnean Society* 103: 336-345.

Mendez, C., C. Stern, O. Reyes and F. Mena (2012) Early Holocene Long Distance Obsidian Transport in Central-south Patagonia. *Chungara, Revista de Antropología Chilena* 44(3): 363-375.

Stern, C. (1999). Black Obsidian from Central-south Patagonia: Chemical Characteristics, Sources and Regional Distribution of Artifacts. *Soplando en el viento. Actas de las III Jornadas de Arqueologia de la Patagonia*, pp. 221-234.

Stern, C. and N. V. Franco (2000) Obsidiana Gris Verdosa Veteada de la Cuenca Superior del Rio Santa Cruz, Extremo Sur de Patagonia. *Anales del Instituto de la Patagonia*, Serie Ciencias Humanas 28: 265-273.

Stern, C., J. Gomez Otero and J. B. Belardi (2000) Características Químicas, Fuentes Potenciales y Distribución de Diferentes Tipos de Obsidiana en el Norte de la Provincia del Chubut, Patagonia Argentina. *Anales del Instituto de la Patagonia*, Serie Ciencias Humanas 28: 275-290

Stern, C., Cruz, I., S. Caracotche, J. Charlin (2012) Grey Porphiritic Obsidian from Chaitén Volcano Found South of the Santa Cruz River in Southernmost Patagonia. *Magallania* 40: 135-142.

Vásquez, C. A., H.G. Nami and A. E. Rapalini (2001) Magnetic Sourcing of Obsidians in Southern South America. *Journal of Archaeological Science* 28(6): 613-618.

ABOUT OUR WEB SITE

The IAOS maintains a website at http://members.peak.org/~obsidian/
The site has some great resources available to the public, and our webmaster, Craig Skinner, continues to update the list of publications and must-have volumes.

You can now become a member online or renew your current IAOS membership using PayPal. Please take advantage of this opportunity to continue your support of the IAOS.

Other items on our website include:

- World obsidian source catalog
- Back issues of the *Bulletin.*
- An obsidian bibliography
- An obsidian laboratory directory
- Photos and maps of some source locations
- Links

Thanks to Craig Skinner for maintaining the website. Please check it out!

CALL FOR ARTICLES

Submissions of articles, short reports, abstracts, or announcements for inclusion in the *Bulletin* are always welcome. We accept electronic media on CD in MS Word. Tables should be submitted as Excel files and images as .jpg files. Please use the *American Antiquity* style guide for formatting references and bibliographies.
http://www.saa.org/Portals/0/SAA/Publications/StyleGuide/StyleGuide_Final_813.pdf

Submissions can also be emailed to the *Bulletin* at IAOS.Editor@gmail.com Please include the phrase "IAOS Bulletin" in the subject line. An acknowledgement email will be sent in reply, so if you do not hear from us, please email again and inquire.

Deadline for Issue #58 is December 1, 2017.

Email or mail submissions to:

Dr. Carolyn Dillian
IAOS Bulletin, Editor
Department of Anthropology & Geography
Coastal Carolina University
P.O. Box 261954
Conway, SC 29528
U.S.A.

Inquiries, suggestions, and comments about the *Bulletin* can be sent to IAOS.Editor@gmail.com
Please send updated address information to Matt Boulanger at Boulanger.Matthew@gmail.com

MEMBERSHIP

The IAOS needs membership to ensure success of the organization. To be included as a member and receive all of the benefits thereof, you may apply for membership in one of the following categories:

Regular Member: $20/year*
Student Member: $10/year or FREE with submission of a paper to the *Bulletin* for publication. Please provide copy of current student identification.
Lifetime Member: $200

Regular Members are individuals or institutions who are interested in obsidian studies, and who wish to support the goals of the IAOS. Regular members will receive any general mailings; announcements of meetings, conferences, and symposia; the *Bulletin*; and papers distributed by the IAOS during the year. Regular members are entitled to vote for officers.

*Membership fees may be reduced and/or waived in cases of financial hardship or difficulty in paying in foreign currency. Please complete the form and return it to the Secretary-Treasurer with a short explanation regarding lack of payment.

NOTE: Because membership fees are very low, the IAOS asks that all payments be made in U.S. Dollars, in international money orders, or checks payable on a bank with a U.S. branch. Otherwise, please use PayPal on our website to pay with a credit card.
http://members.peak.org/~obsidian/

For more information about membership in the IAOS, contact our Secretary-Treasurer:

Matthew Boulanger
Department of Anthropology
Southern Methodist University
P.O. Box 750336
Dallas, TX 75275-0336
U.S.A.
Boulanger.Matthew@gmail.com

Membership inquiries, address changes, or payment questions can also be emailed to Boulanger.Matthew@gmail.com

ABOUT THE IAOS

The International Association for Obsidian Studies (IAOS) was formed in 1989 to provide a forum for obsidian researchers throughout the world. Major interest areas include: obsidian hydration dating, obsidian and materials characterization ("sourcing"), geoarchaeological obsidian studies, obsidian and lithic technology, and the prehistoric procurement and utilization of obsidian. In addition to disseminating information about advances in obsidian research to archaeologists and other interested parties, the IAOS was also established to:

1. Develop standards for analytic procedures and ensure inter-laboratory comparability.
2. Develop standards for recording and reporting obsidian hydration and characterization results
3. Provide technical support in the form of training and workshops for those wanting to develop their expertise in the field.
4. Provide a central source of information regarding the advances in obsidian studies and the analytic capabilities of various laboratories and institutions

MEMBERSHIP RENEWAL FORM

We hope you will continue your membership. Please complete the renewal form below.

NOTE: You can now renew your IAOS membership online! Please go to the IAOS website at http://members.peak.org/~obsidian/ and check it out! Please note that due to changes in the membership calendar, your renewal will be for the next calendar year. Unless you specify, the *Bulletin* will be sent to you as a link to a .pdf available on the IAOS website.

___ Yes, I'd like to renew my membership. A check or money order for the annual membership fee is enclosed (see below).

___ Yes, I'd like to become a new member of the IAOS. A check or money order for the annual membership fee is enclosed (see below). Please send my first issue of the IAOS *Bulletin*.

___ Yes, I'd like to become a student member of the IAOS. I have enclosed either an obsidian-related article for publication in the IAOS *Bulletin* or an abstract of such an article published elsewhere. I have also enclosed a copy of my current student ID. Please send my first issue of the IAOS *Bulletin.*

NAME: ____

TITLE: ____________________ AFFILIATION: ________________________

STREET ADDRESS: ____

CITY, STATE, ZIP: ____

COUNTRY: ____

WORK PHONE: ____________________ FAX: ____________________

HOME PHONE (OPTIONAL): ________________________________

EMAIL ADDRESS: ____

My check or money order is enclosed for the following amount (please check one):
___ $20 Regular
___ $10 Student (include copy of student ID)
___ FREE Student (include copy of article for the *IAOS Bulletin* and student ID)
___ $200 Lifetime

Please return this form with payment: (or pay online with PayPal http://members.peak.org/~obsidian/)

Matthew Boulanger
Department of Anthropology
Southern Methodist University
P.O. Box 750336
Dallas, TX 75275-0336
U.S.A.